



Preparation of cluster-like nanostructure and nanoribbon for $4\text{ZnO}\cdot\text{B}_2\text{O}_3\cdot\text{H}_2\text{O}$ and the evaluation of their flame retardant properties by a thermal analysis method

Yin-Yan Zhang, Lin Xue, Zhi-Hong Liu*

Key Laboratory for Macromolecular Science of Shaanxi Province, School of Chemistry and Materials Science, Shaanxi Normal University, Xi'an 710062, China

ARTICLE INFO

Article history:

Received 28 January 2010

Received in revised form 17 April 2010

Accepted 22 April 2010

Available online 29 April 2010

Keywords:

Nanomaterials

Zinc borate

Hydrothermal preparation

Flame retardant property

Thermal analysis

ABSTRACT

Cluster-like $4\text{ZnO}\cdot\text{B}_2\text{O}_3\cdot\text{H}_2\text{O}$ nanostructure and $4\text{ZnO}\cdot\text{B}_2\text{O}_3\cdot\text{H}_2\text{O}$ nanoribbon have been prepared under hydrothermal conditions at 120°C for 12 h. All the samples were characterized by the X-ray powder diffraction (XRD), infrared spectrum (IR), and energy dispersive X-ray spectroscopy (EDS). The sizes and morphologies of the products were investigated by scanning electron microscope (SEM) and transmission electron microscope (TEM). The results show that $4\text{ZnO}\cdot\text{B}_2\text{O}_3\cdot\text{H}_2\text{O}$ cluster consists of nanoribbons with the thickness of about 80 nm and the width of 200–300 nm. $4\text{ZnO}\cdot\text{B}_2\text{O}_3\cdot\text{H}_2\text{O}$ nanoribbon is about 50 nm in thickness and about 200–500 nm in width. The flame retardant properties of the prepared $4\text{ZnO}\cdot\text{B}_2\text{O}_3\cdot\text{H}_2\text{O}$ nanomaterials were investigated by the thermal analysis method and a vertical combustion test, demonstrating that they had the better behaviors than the non-nanostructure sample.

© 2010 Elsevier B.V. All rights reserved.

1. Introduction

There are many kinds of zinc borates [1] found in nature as well as synthesized in the laboratory. Some of these borates have useful properties. For example, zinc borates with different chemical formula such as $2\text{ZnO}\cdot 3\text{B}_2\text{O}_3\cdot 3.5\text{H}_2\text{O}$, $4\text{ZnO}\cdot\text{B}_2\text{O}_3\cdot\text{H}_2\text{O}$, and $2\text{ZnO}\cdot 3\text{B}_2\text{O}_3$ are the fire retardant materials used in plastics [2]. However, the zinc borate particles are hardly dispersed in a polymer matrix, which restrains their uses in industry. Besides the sizes, the morphologies of a fire retardant also greatly affect its fire retardant property. Therefore, much attention has been paid to the application of nanometer particles. To date, there are only a few reports on the preparation of zinc borates with nanostructures, such as ZnB_4O_7 nanotubes [3] and $\text{Zn}_2\text{B}_6\text{O}_{11}\cdot 3\text{H}_2\text{O}$ nanodiscs [4]. Recently, Yuan and coworkers [5,6] have reported $4\text{ZnO}\cdot\text{B}_2\text{O}_3\cdot\text{H}_2\text{O}$ nano-/microstructures with different morphologies (rod-, wire-, and lamellar-like shapes and microspheres of nano-/microrods) prepared by a PEG-300 assisted hydrothermal method. But their flame retardant properties were not evaluated.

In this paper, we report the preparation of two new morphologies—a cluster-like $4\text{ZnO}\cdot\text{B}_2\text{O}_3\cdot\text{H}_2\text{O}$ nanostructure and a $4\text{ZnO}\cdot\text{B}_2\text{O}_3\cdot\text{H}_2\text{O}$ nanoribbon—under hydrothermal conditions, and the evaluation of their flame retardant properties by a thermal analysis method.

2. Experimental

2.1. Preparation of samples

All the chemical reagents used in our experiments were of analytical grade and were used without further purification.

For cluster-like $4\text{ZnO}\cdot\text{B}_2\text{O}_3\cdot\text{H}_2\text{O}$ nanostructure sample: the mixture of 0.60 g of $\text{ZnSO}_4\cdot 7\text{H}_2\text{O}$, 0.12 g of sodium bis(2-ethylhexyl) sulfosuccinate (AOT), 2.0 g of KNO_3 , 10.0 mL of deionized water and 10.0 mL of ethanol was stirred at 50°C until homogeneous. Then 10.0 mL of 0.2 mol L^{-1} borax aqueous solution was added dropwise to the above mixture while being stirred for 0.5 h. The final mixture with $\text{pH}=6.0$ was transferred into a 40 mL Teflon-lined stainless autoclave. For $4\text{ZnO}\cdot\text{B}_2\text{O}_3\cdot\text{H}_2\text{O}$ nanoribbon sample: 0.95 g borax and 0.9 g boric acid were dissolved in 25 mL of distilled water to give solution A, and 0.71 g $\text{ZnSO}_4\cdot 7\text{H}_2\text{O}$ was dissolved in 15 mL of distilled water to give solution B. Both solutions were placed in ultrasonic bath and sonicated at 59 kHz for 30 min. Then the solution B was poured into the solution A slowly, forming a homogeneous mixture which was continued to sonicated for another 60 min. After being added 20 mL of distilled water, the obtained mixture was transferred into a 100 mL Teflon-lined stainless autoclave. The above two autoclaves were maintained at 120°C for 12 h under autogenous pressure and then cooled to room temperature. The resulting white precipitates were obtained by filtration, washed 3 times respectively with deionized water and anhydrous ethanol, and dried in air at 60°C for 8 h, which were collected for the following characterization.

* Corresponding author. Tel.: +86 29 8530 7765; fax: +86 29 8530 7774.
E-mail address: liuzh@snnu.edu.cn (Z.-H. Liu).

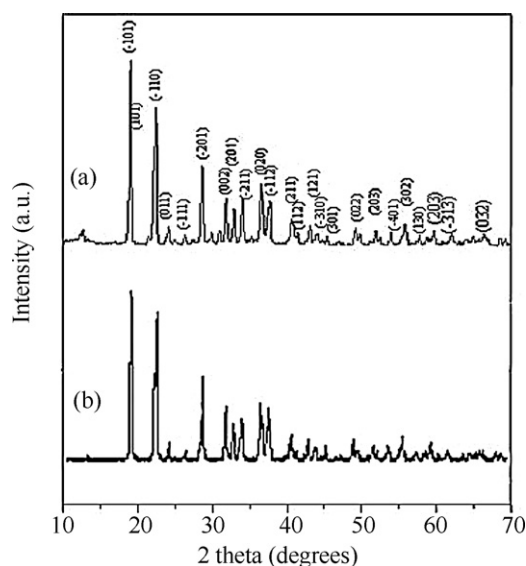


Fig. 1. XRD patterns of samples: (a) cluster-like nanostructure; (b) nanoribbon.

2.2. Characterization of the samples

All samples were identified by X-ray powder diffraction (XRD; recorded on a Rigaku D/MAX-IIIIC with Cu target at a scanning rate of 8° min^{-1} with 2θ ranging from 10° to 70°), FT-IR spectroscopy (Nicolet NEXUS 670 FT-IR spectrometer in the range of $400\text{--}4000 \text{ cm}^{-1}$ with KBr pellets at room temperature) and the energy dispersive X-ray spectroscopy (EDS) attached to the following SEM. The sizes and morphologies of the products were investigated by scanning electron microscope (SEM; Quanta 200, Philips-FEI; before SEM imaging, the sample was coated with thin layers of gold) and transmission electron microscope (TEM; Hitachi H-600).

2.3. Flame retardant evaluation

The flame retardant properties of samples were investigated through the thermal analysis method. Wood powder was selected as the blank sample. 20% prepared samples and non-nanostructure sample of $4\text{ZnO}\cdot\text{B}_2\text{O}_3\cdot\text{H}_2\text{O}$ were added into the selected wood powder, and the mixtures were stirred until homogeneous, respectively. The thermogravimetric analysis (TGA) of the obtained mixture samples was performed on an SDT Q600 thermal analyzer under N_2 atmosphere with a heating rate of $20^\circ \text{ C min}^{-1}$.

3. Results and discussion

3.1. Characterization of $4\text{ZnO}\cdot\text{B}_2\text{O}_3\cdot\text{H}_2\text{O}$ samples

Fig. 1 gives the XRD patterns of the prepared $4\text{ZnO}\cdot\text{B}_2\text{O}_3\cdot\text{H}_2\text{O}$ samples. The data of XRD pattern of the prepared nanoribbon sample and corresponding data in the literature [5] are listed in Table 1. The main characteristic d values of the $4\text{ZnO}\cdot\text{B}_2\text{O}_3\cdot\text{H}_2\text{O}$ samples corresponded with those of the reported data in the literature [5,6] and the patent [7]. Furthermore, EDS analysis (Fig. 2) indicates the presence of Zn, B and O atoms.

The FT-IR spectra (Fig. 3) of the $4\text{ZnO}\cdot\text{B}_2\text{O}_3\cdot\text{H}_2\text{O}$ samples exhibited the following absorption bands and they were assigned referring to the literature [8]. The band at 3458 cm^{-1} is the stretching of O–H. The peaks at 1380 and 1306 cm^{-1} might be asymmetric and symmetric stretching of $\text{B}_{(3)}\text{--O}$, respectively. The peaks at 1242 and 1119 cm^{-1} are the in-plane bending of B–O–H. The strong peak

Table 1

XRD data of prepared sample and corresponding values in the literature [5].

Measured values			Values in the literature [5]		
$2\theta/^\circ$	$d/\text{\AA}$	hkl	$2\theta/^\circ$	$d/\text{\AA}$	hkl
18.74	4.7310	100	18.81	4.7141	100
21.92	4.0514	51	21.94	4.048	62
22.20	4.0011	88	22.25	3.9923	68
23.88	3.7232	10	23.95	3.7131	9
26.18	3.4014	6	26.14	3.4058	5
28.44	3.1357	49	28.47	3.1329	48
31.68	2.8223	32	31.73	2.8206	35
32.72	2.7349	20	32.73	2.7342	20
33.80	2.6495	23	33.87	2.6442	28
36.36	2.4688	33	36.43	2.4641	33
37.30	2.4087	20	37.31	2.4082	21
37.54	2.3939	32	37.60	2.3904	32
40.70	2.2151	13	40.77	2.2113	15
41.36	2.1814	6	41.29	2.1848	7
42.92	2.1055	12	42.90	2.1062	15
43.90	2.0607	7	43.91	2.0601	9
45.26	2.0018	8	45.27	2.0014	8
49.06	1.8554	12	49.07	1.8551	14
49.72	1.8323	5	49.75	1.8311	7
51.74	1.7654	7	51.77	1.7644	11
52.34	1.7466	5	52.35	1.7464	6
53.82	1.7019	8	53.85	1.7011	10
55.80	1.6461	14	55.81	1.6458	17
59.60	1.5499	9	59.65	1.5487	12
61.90	1.4977	5	61.96	1.4966	7
66.52	1.4046	5	66.36	1.4075	7
66.79	1.3995	5	66.77	1.3999	5

at 716 cm^{-1} is the out-of-plane bending of $\text{B}_{(3)}\text{--O}$. The peaks at 534 cm^{-1} is the in-plane bending of $\text{B}_{(3)}\text{--O}$. The peaks at 1028 and 475 cm^{-1} might be the vibration of Zn–O [9]. These assignments reveal the presence of triangular BO_3 and OH groups in this compound, which are consistent with the structure of $\text{Zn}_2(\text{OH})\text{BO}_3$ [10].

3.2. Size and morphology of $4\text{ZnO}\cdot\text{B}_2\text{O}_3\cdot\text{H}_2\text{O}$ samples

The lower magnification and higher magnification SEM images and TEM images of the samples for cluster-like $4\text{ZnO}\cdot\text{B}_2\text{O}_3\cdot\text{H}_2\text{O}$ nanostructure and $4\text{ZnO}\cdot\text{B}_2\text{O}_3\cdot\text{H}_2\text{O}$ nanoribbons are shown in Figs. 4 and 5, respectively. Both the morphology and size determined by TEM are similar to the SEM images. Fig. 4(a) and (b) shows that cluster-like $4\text{ZnO}\cdot\text{B}_2\text{O}_3\cdot\text{H}_2\text{O}$ nanostructure consists of nanoribbons with the thickness of about 80 nm, the width of

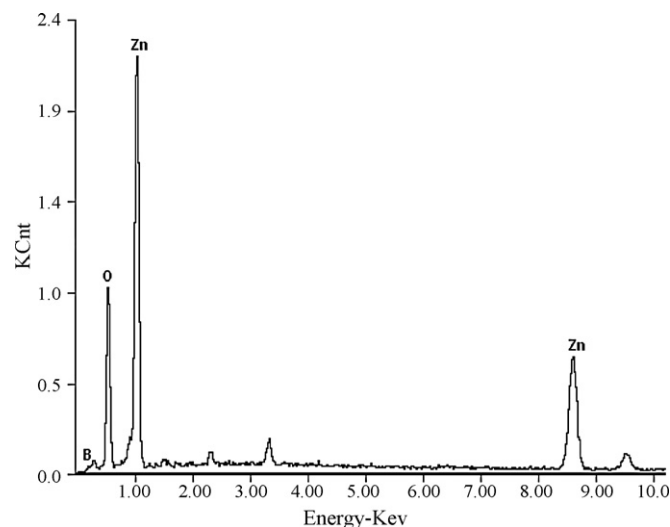


Fig. 2. EDS spectrum of prepared $4\text{ZnO}\cdot\text{B}_2\text{O}_3\cdot\text{H}_2\text{O}$ sample.

200–300 nm, and length up to several micrometers. Furthermore, we also observed that these clusters are intersections to each other. As is shown in Fig. 4(c) and (d), the uniform $4\text{ZnO}\cdot\text{B}_2\text{O}_3\cdot\text{H}_2\text{O}$ nanoribbons were about 50 nm in thickness and about 200–500 nm in width. As a comparison, the SEM images of the $4\text{ZnO}\cdot\text{B}_2\text{O}_3\cdot\text{H}_2\text{O}$ non-nanostructure sample are also given in Fig. 4, which shows that it is the irregular blocks with about 1–5 μm in width and about 1–2 μm in thickness.

3.3. The possible formation mechanism of cluster-like $4\text{ZnO}\cdot\text{B}_2\text{O}_3\cdot\text{H}_2\text{O}$ nanostructure

Based on the experimental results, it could be concluded that the formation of such cluster-like $4\text{ZnO}\cdot\text{B}_2\text{O}_3\cdot\text{H}_2\text{O}$ nanostructure is achieved via a self-assembly process.

$4\text{ZnO}\cdot\text{B}_2\text{O}_3\cdot\text{H}_2\text{O}$ nanoribbons were firstly formed through conventional nucleation and subsequent crystal growth process. The possible reactions are as follows:

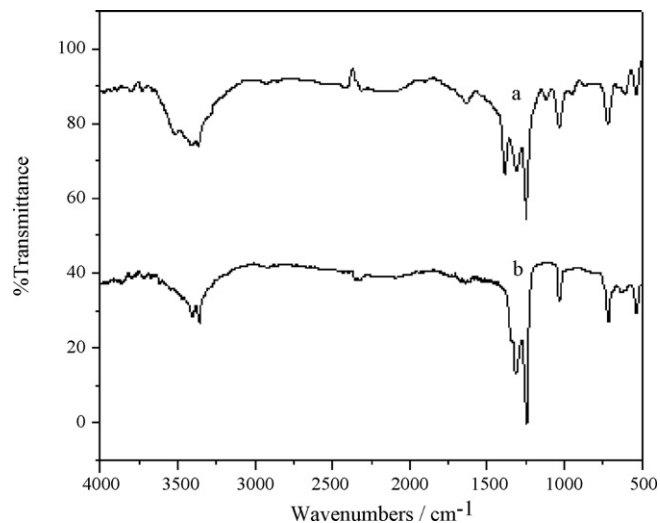
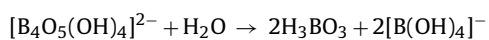


Fig. 3. FT-IR spectra of samples: (a) cluster-like nanostructure; (b) nanoribbon.

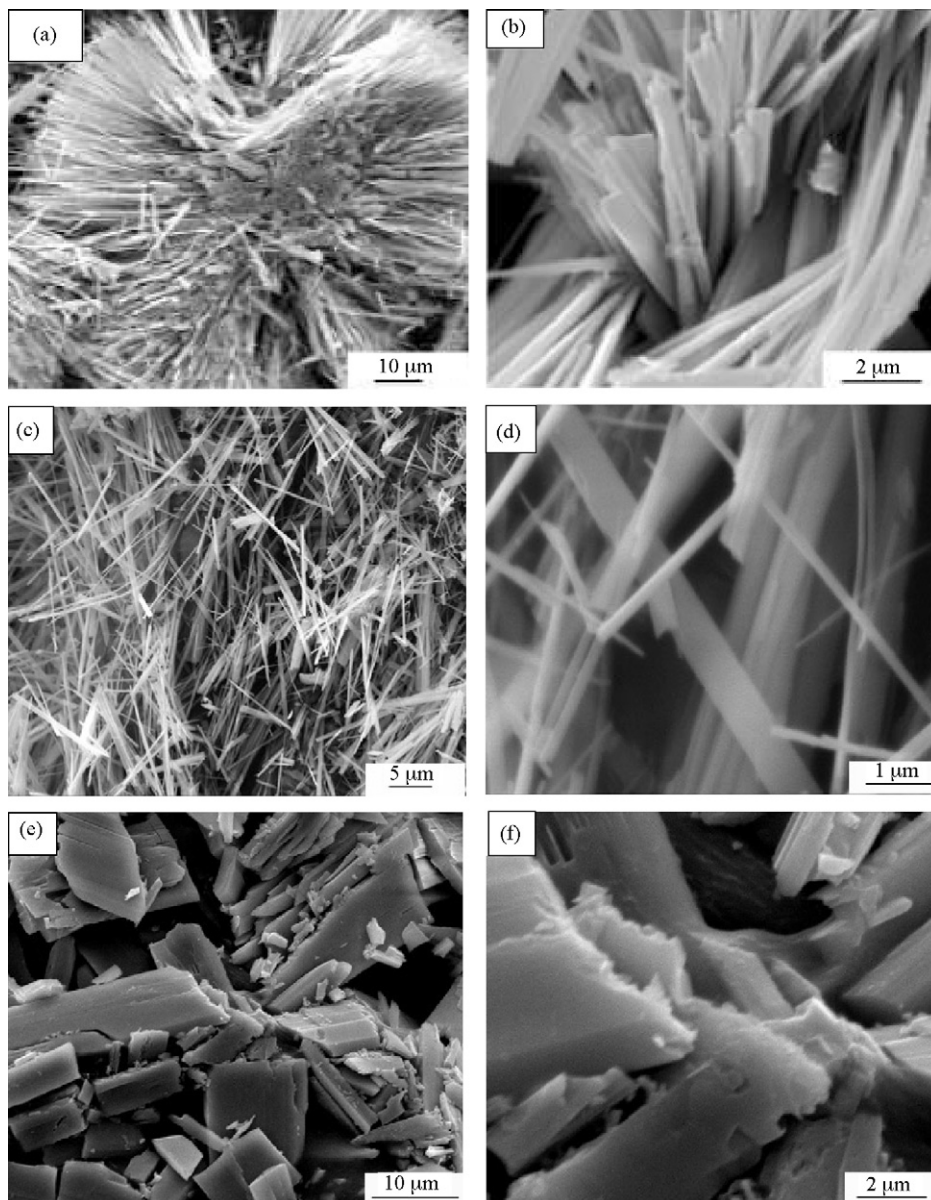


Fig. 4. The SEM images of samples: (a) and (b) cluster-like nanostructure; (c) and (d) nanoribbon; (e) and (f) non-nanostructure sample.

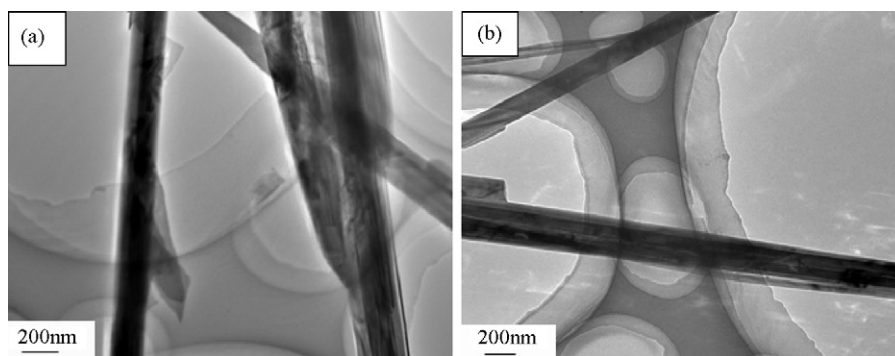
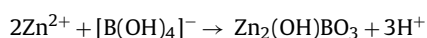


Fig. 5. The TEM images of samples: (a) cluster-like nanostructure; (b) nanoribbon.



Then, AOT might provide a soft template for self-assembly process, which could adsorb the nanoribbons selectively, and further tended to aggregate forming cluster in order to lower the surface energy by reducing exposed areas. This is consistent with the fact that no cluster-like $4\text{ZnO} \cdot \text{B}_2\text{O}_3 \cdot \text{H}_2\text{O}$ nanostructure was formed in the absence of AOT in our experiment. In addition, it was the existing positive and negative electric charge in AOT that possibly resulted in the intersections in the clusters.

3.4. Flame retardant properties

Fig. 6 shows TG curves of wood powder, wood powder with 20% non-nanostructure sample of $4\text{ZnO} \cdot \text{B}_2\text{O}_3 \cdot \text{H}_2\text{O}$, and wood powder with 20% prepared samples of cluster-like $4\text{ZnO} \cdot \text{B}_2\text{O}_3 \cdot \text{H}_2\text{O}$ nanostructure and $4\text{ZnO} \cdot \text{B}_2\text{O}_3 \cdot \text{H}_2\text{O}$ nanoribbon, respectively. The corresponding mass losses at different temperatures are listed in Table 2. As shown in Fig. 6, all the samples had a two-step mass losses between 30 and 700 °C. The first mass losses at 30–150 °C correspond to the loss of adsorbed water in wood powder. The second mass losses at 150–700 °C correspond to the decomposition of wood. From Fig. 6 and Table 2, it can be seen that the final mass losses at 700 °C are gradually decreased, namely, 92.56% for a, 77.04% for b, and 75.75% for c, and 70.59% for d. Furthermore, the mass losses at any same temperatures are also gradually decreased

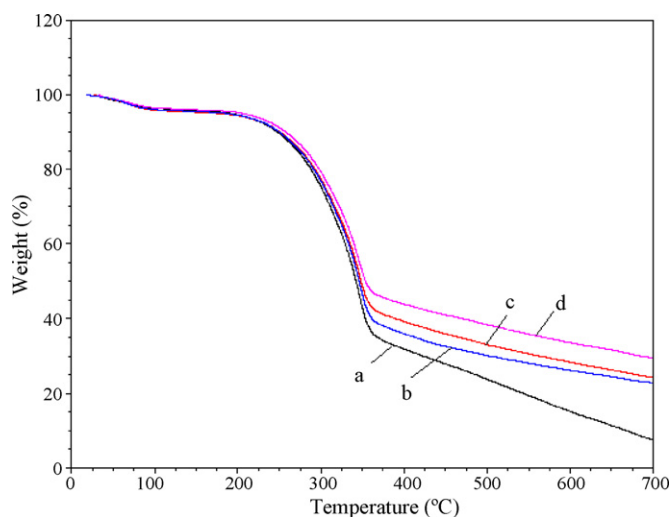


Fig. 6. TG curves of samples: (a) wood powder; (b) wood powder with 20% $4\text{ZnO} \cdot \text{B}_2\text{O}_3 \cdot \text{H}_2\text{O}$ non-nanostructure sample; (c) wood powder with 20% prepared cluster-like $4\text{ZnO} \cdot \text{B}_2\text{O}_3 \cdot \text{H}_2\text{O}$ nanostructure sample; (d) wood powder with 20% prepared $4\text{ZnO} \cdot \text{B}_2\text{O}_3 \cdot \text{H}_2\text{O}$ nanoribbon sample.

Table 2

Mass losses (%) at different temperatures in TG curves.^a

Samples	T/°C				
	300	400	500	600	700
a	24.90	68.14	75.29	84.92	92.56
b	23.17	63.82	69.70	73.71	77.04
c	22.80	60.74	66.93	71.67	75.75
d	20.89	56.09	61.59	66.40	70.59

^a (a) Wood powder; (b) wood powder with 20% $4\text{ZnO} \cdot \text{B}_2\text{O}_3 \cdot \text{H}_2\text{O}$ non-nanostructure sample; (c) wood powder with 20% prepared cluster-like $4\text{ZnO} \cdot \text{B}_2\text{O}_3 \cdot \text{H}_2\text{O}$ nanostructure sample; (d) wood powder with 20% prepared $4\text{ZnO} \cdot \text{B}_2\text{O}_3 \cdot \text{H}_2\text{O}$ nanoribbon sample.

Table 3

The result of vertical combustion test.^a

Samples	Duration of flame application/s	Duration of after flame/s	Duration of afterglow/s
a	12	29.7	149.5
b	12	25.9	93.8
c	12	22.8	83.9
d	12	21.6	82.4

^a (a) Wood powder; (b) wood powder with 20% $4\text{ZnO} \cdot \text{B}_2\text{O}_3 \cdot \text{H}_2\text{O}$ non-nanostructure sample; (c) wood powder with 20% prepared cluster-like $4\text{ZnO} \cdot \text{B}_2\text{O}_3 \cdot \text{H}_2\text{O}$ nanostructure sample; (d) wood powder with 20% prepared $4\text{ZnO} \cdot \text{B}_2\text{O}_3 \cdot \text{H}_2\text{O}$ nanoribbon sample.

from samples a to d, indicating that the decomposing rates are gradually decreased from samples a to d. This result shows that the flame retardant properties of cluster-like $4\text{ZnO} \cdot \text{B}_2\text{O}_3 \cdot \text{H}_2\text{O}$ nanostructure and $4\text{ZnO} \cdot \text{B}_2\text{O}_3 \cdot \text{H}_2\text{O}$ nanoribbon samples are better than that of non-nanostructure one, and the flame retardant property of $4\text{ZnO} \cdot \text{B}_2\text{O}_3 \cdot \text{H}_2\text{O}$ nanoribbon sample is better than that of cluster-like $4\text{ZnO} \cdot \text{B}_2\text{O}_3 \cdot \text{H}_2\text{O}$ nanostructure sample, which can be ascribed to the less thickness of nanoribbon.

As a comparison, we also evaluated the flame retardant properties of prepared samples by a vertical combustion tester (ZBY-1, China). All the tested samples were stirred until homogeneous, and then were pressed into pieces. The results of vertical combustion test are shown in Table 3. It can be seen that the duration of after flame and the duration of afterglow are all gradually decreased from samples a to d at the same duration of flame application. This result shows that the flame retardant properties are gradually improved from non-nanostructure $4\text{ZnO} \cdot \text{B}_2\text{O}_3 \cdot \text{H}_2\text{O}$ to cluster-like $4\text{ZnO} \cdot \text{B}_2\text{O}_3 \cdot \text{H}_2\text{O}$ nanostructure and to $4\text{ZnO} \cdot \text{B}_2\text{O}_3 \cdot \text{H}_2\text{O}$ nanoribbon sample, which corresponds with the result of above TGA test.

4. Conclusions

In summary, cluster-like nanostructure and nanoribbon for $4\text{ZnO} \cdot \text{B}_2\text{O}_3 \cdot \text{H}_2\text{O}$ have been prepared under hydrothermal condi-

tions at 120 °C for 12 h. The flame retardant tests, including the TGA method and the vertical combustion method, showed that the prepared $4\text{ZnO}\cdot\text{B}_2\text{O}_3\cdot\text{H}_2\text{O}$ nanomaterials had the better behavior than the non-nanostructure sample, and the $4\text{ZnO}\cdot\text{B}_2\text{O}_3\cdot\text{H}_2\text{O}$ nanoribbon sample had the better behavior than the cluster-like nanostructure sample, which showed that the evaluation of flame retardant property of nanomaterials by thermal analysis method was feasible.

Acknowledgments

Project was supported by the National Natural Science Foundation of China (No. 20871078) and the Natural Science Foundation of Shaanxi Province of China (No. SJ08B01).

References

- [1] D.M. Schubert, F. Alam, M.Z. Visi, C.B. Knobler, *Chem. Mater.* 15 (2003) 866.
- [2] A. Mergen, E. Tektas, G. Karakoc, M. Gunduz, *Ceram. Forum Int.* 80 (2003) 40.
- [3] J.B. Chang, P.X. Yan, Q. Yang, *J. Cryst. Growth* 286 (2006) 184.
- [4] Y.M. Tian, Y.P. Guo, M. Jiang, Y. Sheng, B.L. Hari, G.Y. Zhang, B. Zhou, Y.C. Zhu, Z.C. Wang, *Mater. Lett.* 60 (2006) 2511.
- [5] X.X. Shi, M. Li, H. Yang, S.P. Chen, L.J. Yuan, K.L. Zhang, J.T. Sun, *Mater. Res. Bull.* 42 (2007) 1649.
- [6] X.X. Shi, L.J. Yuan, X.Z. Sun, C.X. Chang, J.T. Sun, *J. Phys. Chem. C* 112 (2008) 3558.
- [7] D.M. Shubert, US Patent 5,342,553 (1994).
- [8] J. Li, S.P. Xia, S.Y. Gao, *Spectrochim. Acta* 51A (1995) 519.
- [9] M.N. Liu, G.Q. Wang, C. Luo, Y. Xu, *Fine Chem. Intermediates* 32 (2002) 34.
- [10] Z.T. Yu, J.J. Xu, Y.S. Jiang, Z. Shi, Y. Guo, D.J. Wang, J.S. Chen, *J. Mater. Chem.* 13 (2003) 2227.